Laser surface hardening: a review

P. Dinesh Babu and K.R. Balasubramanian*

Department of Mechanical Engineering,
National Institute of Technology,
Tiruchirappalli-620015, India
Fax: +91-431-2500133
E-mail: pdineshbabu81@gmail.com
E-mail: krbala@nitt.edu
*Corresponding author

G. Buvanashekaran

Welding Research Institute,
Bharat Heavy Electricals Ltd.,
Tiruchirappalli-620014, India
Fax: +91-431-2500133
E-mail: gbs@bheltry.co.in

Abstract: Laser surface hardening (LSH) is one of the most widely used surface hardening process which can be applied to almost the whole range of metallic materials in today's applications. Laser beam is focused to the localised region for hardening the required portion of the material. High intensity laser radiation is involved for heating the surface of steel into the austenitic region. Steep temperature gradient arises, due to high rates of heat transformation that results in instant cooling by conduction. It causes the phase conversion from austenite to martensite without the need for external quenching. Among various types of lasers, CO_2, Nd: YAG and diode lasers are the widely used lasers for hardening in industries. This review paper is a summary of the basic fundamentals of laser hardening, figuring some of its benefits compared with conventional hardening technique. The works published by various researchers by experimentation and by numerical approach are presented.

Keywords: laser surface hardening; LSH; micro hardness; numerical analysis; wear; microstructure.

Reference to this paper should be made as follows: Dinesh Babu, P., Balasubramanian, K.R. and Buvanashekaran, G. (2011) 'Laser surface hardening: a review', *Int. J. Surface Science and Engineering*, Vol. 5, Nos. 2/3, pp.131–151.

Biographical notes: P. Dinesh Babu is a Full Time Research Scholar and is working in the area of laser surface modification in National Institute of Technology, Tiruchirappalli, India. His research interest is laser surface modification.

K.R. Balasubramanian is an Assistant Professor in the Department of Mechanical Engineering, National Institute of Technology (NIT). His research interests include laser materials processing, heat transfer analysis and modelling and simulation.

G. Buvanashekaran is the Senior Deputy General Manager, Laser Materials Processing Division, Welding Research Institute, BHEL. His research interests include high energy beam welding.

1 Introduction

Laser is one of the most important inventions of the 20th century. Rapid advances in laser technology in the past decade made it possible to perform various operations such as heat treating, glazing, alloying, and cladding on surface of materials, resulting in better physical properties of the surface and improved performance in the given environment. As laser is an expensive source of energy, it is used only in cases where it offers some technical and economical benefits compared to conventional methods. Among the non-conventional techniques, laser surface treatment became most popular due to the recent development of high power, neodymium yttrium-aluminium-garnet (Nd: YAG) solid type, CO_2 and diode lasers. These lasers may have pulsed or continuous output power. One important area of surface-treatment is surface hardening. This is an extensively used process in the treatment of surfaces on mechanical parts (Davis, 2002).

In conventional methods of heat treatment the component is heated to the required temperature and then quenched in oil or water to achieve the desired hardness at the surface. In most industrial applications, wear occurs only in selected areas of the component; hence, it is sufficient to harden these areas to enhance the performance of the component. The advantages of using laser for surface processing results from its highly directional nature and the ability to deliver controlled amounts of energy to desired regions. The energy input is dependent on the absorptivity of the material. Only a fraction of the laser energy is absorbed by the material and the remaining portion is reflected from the surface. The absorption of a polished metal surface depends strongly on the wavelength of irradiation. In the case of steels, the absorptivity increases when the wavelength is short. The wave length of Nd: YAG laser beam is 1.064 μm where the CO_2 laser beam is 10.6 μm. So the Nd: YAG laser which is having short wave length is suitable for surface hardening of steel (Grum and Sturm, 1997).

Due to higher wavelength, CO_2 laser offers a low coupling interaction with metallic substances. Before CO_2 laser hardening (LH), painting or coating has to be applied on the base metal to increase the absorption rate. The used paint or coating causes pollution and hazardous effects to the environment. In contrast, Nd: YAG laser is emerging as a competitive tool in surface modification due to the short wavelength and high absorbing rate of the materials and coating of base material is not needed which is the advantage compared to CO_2 laser. A schematic sketch of the Nd: YAG laser surface hardening (LSH) system is shown in Figure 1. The laser energy generated from Nd:YAG laser can be transformed via fibre optic cable to the workplace which is not possible by CO_2 laser. Inert gases Ar, Ne and He are used to avoid atmospheric contamination.

The major advantages of LSH are:

- low energy usage in comparison with conventional surface heat-treatment processes
- energy input can be adjusted in a wide range by changing laser-beam power, with converging lenses having different focuses at different levels of defocus, and by choosing different travel speeds of work piece

- the optical system for beam guidance from the source to the work piece surface can be adjusted to the hardened-layer profile form, i.e., to the exactness of the product, using lenses and mirrors of different shapes
- a hardened surface will be obtained by self-quenching of the heated surface layer
- without any quenching media, the hardening processes are clean and the workpieces need not be cleaned
- beam guidance over the work piece surface can be automated
- heat treatment can be done on small parts
- good reproducibility of the microstructure and profile of the surface-hardened layer.

Some demerits of LSH are as follows

- high initial investment
- surface preparation is needed in some cases
- protection against radiation is required
- highly skilled operators are needed (Grum, 2007).

Figure 1 Schematic sketch of Nd: YAG laser system

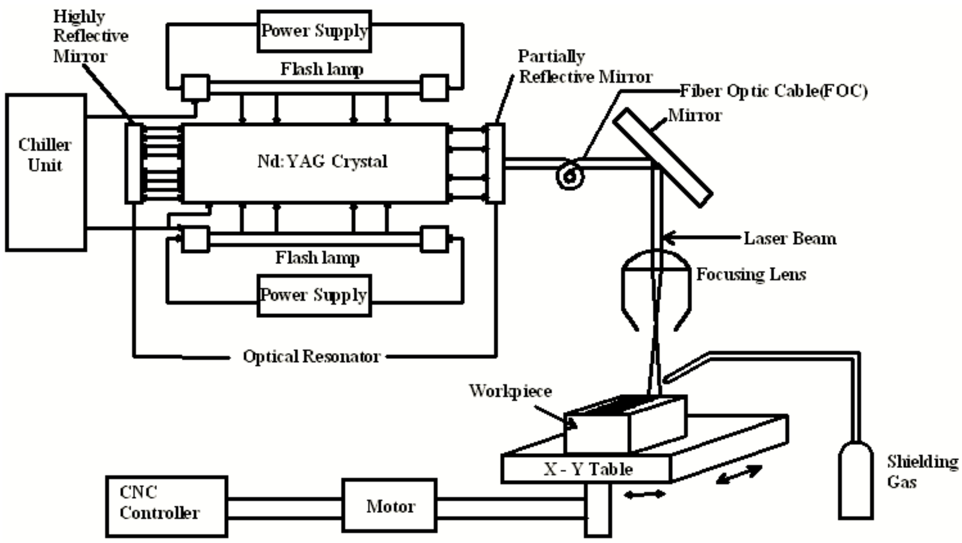

2 Laser surface hardening

In laser heat treatment, laser is used as a heat source where the beam energy is applied to harden a surface on a localised region with the rest of the component acting as a heat sink. As ferrous materials are very good heat conductors, the high heat fluxes generated by lasers are most suitable to heat the surface layer to austenitisation levels without affecting the bulk temperature of the sample. The ensuing self-quenching is rapid enough to eliminate the need for external quenching to produce the hard martensite in the heated surface. Thus, a highly wear resistant surface with the desired core properties of the component can be obtained. Components that have undergone LSH treatments include such highly stressed machine parts such as gears, gear teeth, camshafts, gear housing shafts, cylinder liners, axles, and exhaust valves and valve guides. Many of these applications are in automotive industries, which were among the first mass-production industries to exploit lasers for surface treatments (Totten, 2006).

LSH is a rapid and efficient process for hardening various materials such as tool and die steel, cast iron and medium-carbon steel. Selection of process parameter such as laser power, beam diameter, beam shape, scan velocity, focusing conditions and the shielding gas environment, as well as the material chemistry is important to obtain the desired performance (Yang et al., 1990).

The development of different hardening technologies created new possibilities to form regions with unique properties locally in the materials and to improve the quality of the entire product. Surface transformation hardening of steels is an attractive application of industrial lasers in view of the enormous usage of steel for a numerous applications and the fact that a fine laser beam enables selective hardening to a required depth and width. Of all the applications in laser material processing, LSH is most widely used, well established technique for heat treating the surfaces of steel and competing against the widely used flame and induction hardening methods (Shiue and Chen, 1992).

The LSH process is highly suitable for medium carbon steel and this technique is used to process the precised areas, which mainly depends on the laser beam size, since the processed area is much localised and the conduction of heat transfer into the bulk material that allows the critical cooling rate for the martensitic transformation, without the requirement of a cooling medium. Due to high rate of cooling, hardness rate is also high. For these reasons, LH is becoming the optimal technological solution for the surface heat treatment of small and complex components (Tani et al., 2008).

2.1 Material hardness and wear

To ensure the high hardness and wear resistance of the working surface layers of machine components, it is necessary to use treatment with high concentration energy sources, in particular, laser treatment. The tribological properties and the durability of automobile components such as camshafts, crankshafts, brake drums, internal combustion engine valve and valve seat and gears were improved by this method. One of the traditional methods to increase the wear resistance is induction hardening, which gives a homogenous microstructure with good wear resistance but expensive to implement. To cancel out wear in tribological systems it is not always necessary to provide the entire surface with a wear resistant layer. Depending upon the application, it is sufficient to harden locally the load bearing areas which are subjected to wear. Such areas can be treated properly by a laser, either totally or partially. With the effective use of high power laser sources the peak point of hardenability and fineness in microstructure can be obtained (Slatter et al., 2009).

LH of En18 steel with CO_2 laser with laser power of 1.3 and 1.5 kW, scan velocity 1 m min^{-1} and a beam diameter of 3 mm increased the hardness of the base metal from

250 to 900 HV0.2 and a two-fold increase in wear resistance (Pashby et al., 2003). Hence, the laser surface-hardening technique can be used in the automobile industries to increase the service life of camshafts and crankshafts made of En18 steel.

SeDao et al. (2009) studied the change of crystalline structure and composition of the treated DF-2 cold work tool steel surface layers before and after treatments by energy dispersion spectroscopy (EDX). Their measured microhardness values accurately indicated the performance improvement of the treated surface, which is due to the formation of martensite. Penetration depth of the micro-hardness changes mainly with the laser irradiating parameters that recursively results in different microstructures. This shows that appropriate control of the laser irradiation parameters allowed the fulfilment of highest micro-hardness at the outermost surface. Figure 2 shows the hardness profile for laser-hardened samples at 1.5 and 1.3 kW under a scan speed of 1 m min^{-1} and with a beam diameter of 3 mm.

Figure 2 Hardness profile along depth direction of laser-hardened En18 steel

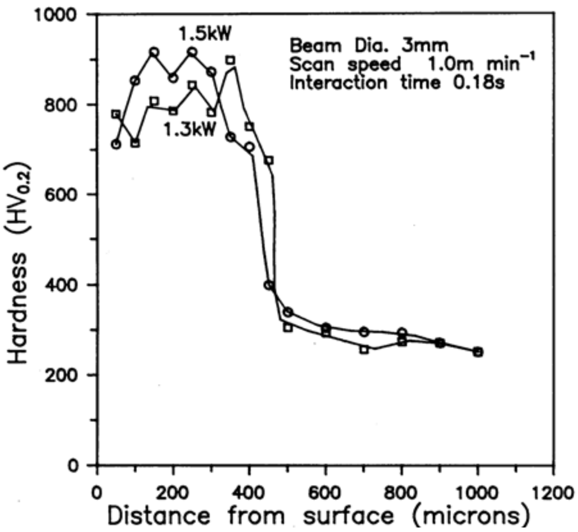

Source: SeDao et al. (2009)

The effect of the Nd:YAG millisecond pulsed laser on the surface morphologies of the irradiated area of DF-2 cold work tool steel using scanning electron microscopy (SEM), EDX and three-dimensional talysurf surface profilometer was investigated by Hua et al. (2007). Results showed that the variation of surface morphology depend on the interaction condition of the laser and the surface during and after surface modification. Furthermore, it has been observed that surface melting or phase transformation occurs due to change in feed rate. Rana et al. (2007) investigated the influence of laser process parameters on the hardness of carbon steel specimen with varying carbon percentage. It was found that when the power is at the intermediate level and the traverse speed is at an optimum value, there was an increase in the hardness. Also, the hardness value increases with decrease in spot laser beam size with slight surface melting, due to enhanced power density which exceeds the critical value. The spot size depends on the width of the hardened zone (HZ) and beam power.

The schematic illustration of laser transformation hardening is shown in Figure 3. The zones between two tracks were considered to be overlapping zones. When the laser heat treatment is required for a large surface area, the overlapping method is used. Optimisation of overlapping of laser HZ was performed by Yang et al. (2006). Conventional overlapping method results in adverse tempering effect and an irregular surface hardness. Softening in overlapping passes by laser scanning is a complex problem of LH. Rana et al. (2007) studied the optimum gap between centre-to-centre distances between the beam overlap regions of laser scanning. They observed that the 2 mm gap between laser beams is more appropriate. There is no significance in reducing the gap below 2 mm in multi-pass laser scanning.

Figure 3 A schematic illustration of laser transformation hardening

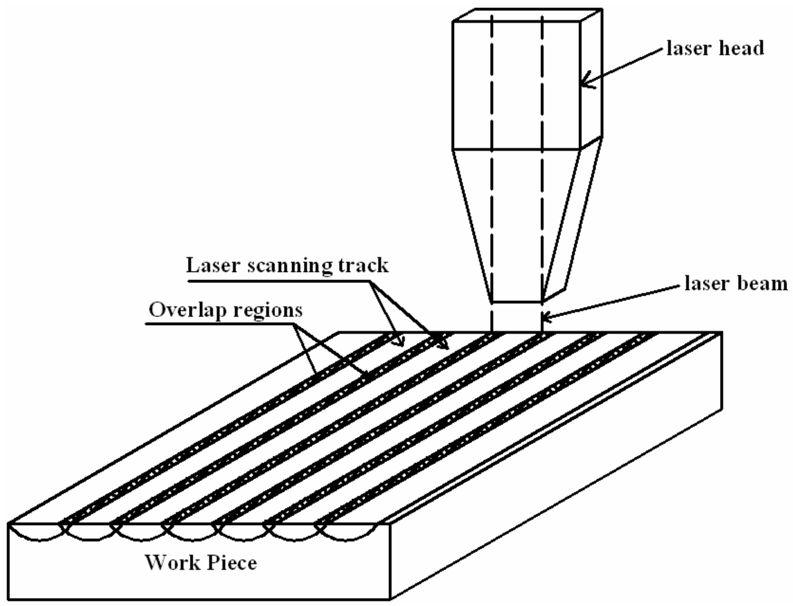

Zhang et al. (1997) investigated the wear, friction characteristics of the CO_2 laser treated surfaces of En31 steel and compared with untreated surfaces with the lubricated ring-on-block technique and analysed the microstructures of the laser-hardened tracks and the worn surfaces by SEM. They observed that the surface of a single hardened track and the surface with two non-overlapping tracks have better wear and friction properties, as compared with the untreated surfaces.

Lakhkar et al. (2008) developed a coupled heat transfer-hardening-tempering model to predict the performance attributes of laser in AISI 4140 steel. The modelling results were validated experimentally. Their work showed that the variation in hardness could be controlled by changing the extent of overlapping of the tracks. Figure 5 shows the result of wear tests made on laser treated and untreated En18 steel specimen employing the pin-on-disc wear testing machine with various sliding forces of 10, 20 and 30 N at room temperature without applying any lubricant. An En24 disc, hardened to 65 Rc, of diameter 150 mm was made to slide against the laser hardened fixed pin, at constant rpm for several hours. The distance travelled by the pin against the rotating disc, that is the change in wear length is converted into sliding distance.

Figure 4 Effect of different multi-pass distances on the variation of micro hardness across a transverse section

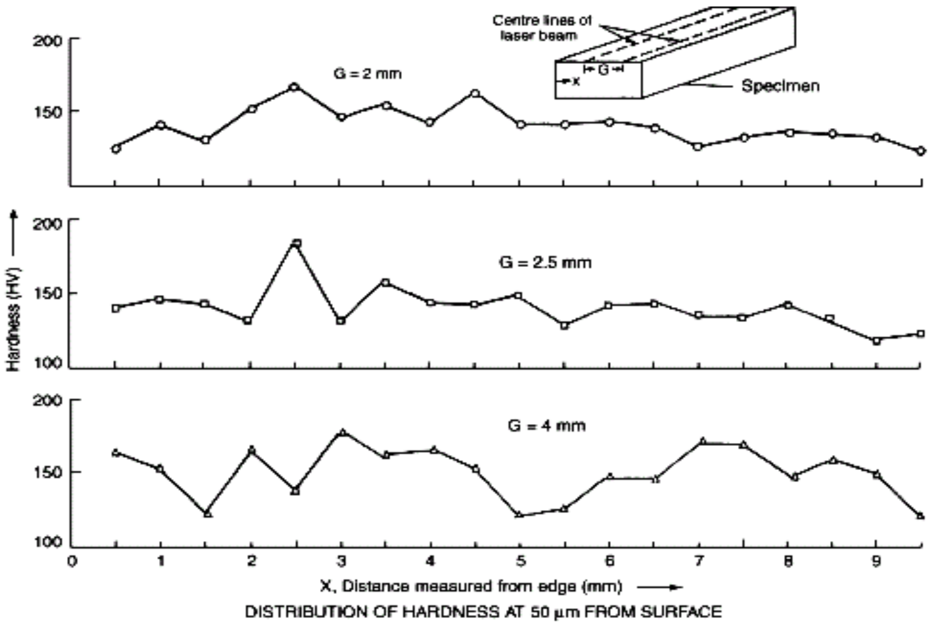

Source: Rana et al. (2007)

Figure 5 Wear curves of laser treated and untreated En18 steel for different load conditions

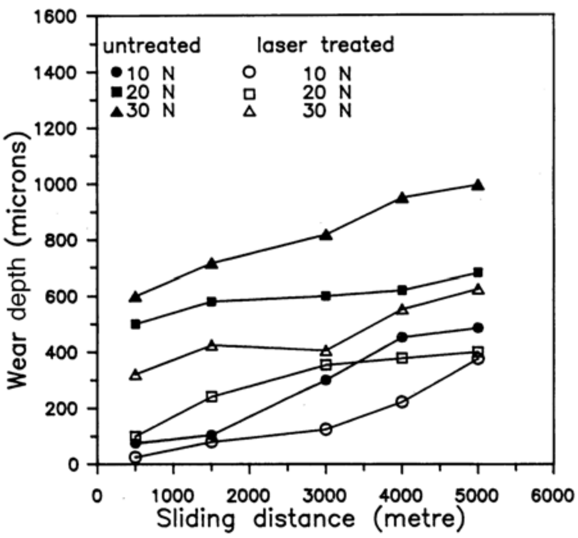

Source: Senthil Selvan et al. (1999)

From Figure 5, it is finalised that untreated specimens have undergone severe wear. The total wear length for a 30 N load at a sliding distance of 5,000 m was 0.9 mm, whereas for the same test conditions the wear length for the laser-hardened specimen was

0.45 mm which shows two-fold increases in the wear resistance. It was that the temperature increase due to friction during the sliding action will further increase the hardness by tempering the martensite to a homogeneous microstructure and thus resulting in good wear resistance. For a sliding distance of 3,000 m, a three-fold increase in wear resistance was obtained for laser hardened samples, but beyond this distance severe wear resulted (Senthil Selvan et al., 1999).

Esa et al. (2007) conducted rolling-sliding wear test on laser hardened silicon and chromium alloyed steel. This machine activates the characterisation and simulation of friction and wear behaviour of the samples. It is found that wear resistance of the surface hardened Si-alloyed steel is better than the wear resistance of the Cr-alloyed steel. The wear coefficient K was defined as

$$K = \frac{V \times H}{P \times S} \tag{1}$$

where V is the volume of wear [m^3] produced in a sliding distance S [mm] under the load P [Kg] and H is the hardness value at the surface. Tianmin et al. (2003) developed ball on flat impact tester to study the impact wear assessment for laser hardened hypoeutectoid 2Cr13 martensite stainless steel. Their results showed that better impact behaviour for 2Cr13 surfaces treated by a continuous wave CO_2 laser than conventional heat treatment. The size of the impact wear scars of 2Cr13 specimens decreases with the increase of the surface hardness.

Wu et al. (2006) reported based on their study that temporal pulse shape has greater effects on hardening parameters. For a rectangular temporal pulse shape, temperature field obtained from model was in agreement with analytical solution. In order to attain the required hardening quality under spatial intensity distribution, the temporal pulse shape should be selected in accordance with pulse energy level. Yang et al. (1991) studied the effect of laser surface-hardening on pre hardened steel and soft annealed steel. The results showed that the 'pre-hardened' specimens possess high depth and width of HZs and a higher surface-hardness when compared with the untreated specimens. The tribological moving components in the automobile industry mainly use grey cast iron. Xiu-bo et al. (2007) used Nd: YAG laser for hardening the grey cast iron. The obtained microhardness level in the hardened layer is 700 HV, which is significantly higher than the microhardness of the substrate region which is 200 HV. It shows that the laser surface hardened layers for grey cast iron has good wear resistance under tribological service conditions.

Liu et al. (1998) used a 2 kW continuous wave CO_2 laser for the laser quenching of the groove of the piston head in large diesel engines. The hardness and depth of the laser quenched layer attained 750 HV and 0.59 mm respectively and is substantially higher than that resulting from the high-frequency quenching method. The microstructure of the quenched layer composed of martensite and retained austenite. The wear testing results showed that the wear resistance of laser quenched specimens was 1.3 times more than that of a high frequency quenching specimen. Practical application of laser quenched piston head in diesel power plants showed that it is an effective way to prolong the service life of the piston head in large diesel engines. The wear of the piston ring is a more severe problem in marine diesel engines as it is operated under adverse conditions such as higher power, higher pressure, and higher piston speed. Hwang et al. (2002) found the optimum process parameters for laser surface-hardening to improve the wear life of piston rings. The resultant hardness of the laser-hardened layer is in the range of 840–950 VHN. The hardened layers formed with heat input ranges between 30 and 45 J/mm and satisfied the piston ring application with the minimum effective hardening depth of 0.3 mm. Pin-on-disc wear-test was carried out which showed that the wear life of the laser-hardened layer was almost twice that of the untreated one.

Figure 6 shows the maximum hardness of the steels for varying carbon content. The dotted line shows the hardness of conventional heat treatment. The circle and dark spot represents the LH performed at the scanning rate of 700 and 300 mm/min. The graph showed that the hardness is increased up to a carbon content of 0.6% and maintains after 0.6% and the hardness after laser treatment increased up to 50 HV than conventional one in the case of less than 0.6% of carbon content (Hirogaki et al., 2001).

Figure 6 Relationship between carbon content and maximum hardness

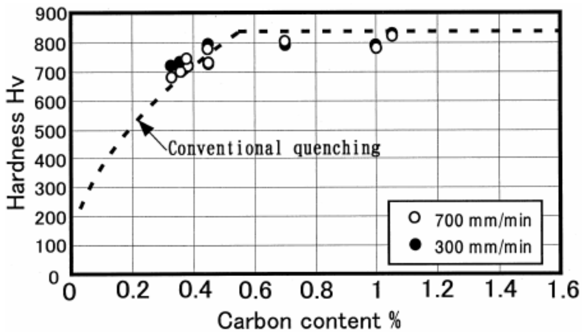

Source: Hirogaki et al. (2001)

Xu et al. (2008) used an infrared process to monitor infrared emissions during LSH of 1,045 steel and grey cast iron using a 1.6 kW pulsed Nd: YAG laser. The signals from the monitor were compared with the hardness and case depth of the laser-treated tracks. Results showed that a linear relationship exists between the monitor output DC level voltage and hardness and the case depth. They found that the infrared process monitoring is also capable of tracking changes in surface quality or flatness of the part that was treated.

The above literature review showed that the material selection, overlap gap and laser type chosen to increase the hardness and wear resistance rate. Optimum overlap gap and process parameters such as scan speed, laser power, beam spot size, are important to increase the hardness and wear resistance.

2.2 Mathematical model

Theoretical models were developed by many researchers to predict the LH. The most important thermophysical characteristic of a material for LH is its thermal diffusivity α, where $\alpha = k/\rho c$ (where k is the thermal conductivity, ρ the density and c the heat capacitance). This factor is involved in all unsteady-state heat flow processes and its importance is that it shows how quickly a material will accept and conduct thermal energy (Ready, 1997). To predict theoretically the temperature field of a laser heat treatment, a number of factors should be taken into account such as: beam intensity profile, the absorption property of the surface, the boundary conditions of work piece and the change in the thermal conductivity with temperature. The time-dependent heat conduction in the space underneath the irradiated surface is described by the following equation (Cheung et al., 2004).

$$\frac{1}{r}\cdot\frac{\partial}{\partial r}\cdot\left(k\cdot r\cdot\frac{\partial T}{\partial r}\right)+\frac{1}{r^2}\cdot\frac{\partial}{\partial\varphi}\cdot\left(k\cdot\frac{\partial T}{\partial\varphi}\right)+\frac{\partial}{\partial z}\left(k\cdot\frac{\partial T}{\partial z}\right)+\dot{q}=\rho\cdot c\cdot\frac{\partial T}{\partial t} \quad (2)$$

where

ρ density (kg/m^3)

c specific heat (J/kg.K)

k thermal conductivity (W/m.K)

T temperature (K)

t time (s)

r, z cylindrical coordinates (m)

φ angle (rad)

$\dot{q}$ rate of energy generation (W/m^3)

Ac_3 the temperature at which, the complete transformation to austenite

Ac_1 the starting temperature at which austenite begins to forms in equilibrium condition.

In the case of conventional hardening the temperature above the Ac_3 line to obtain a homogeneous austenite structure is long enough. Laser beam hardening is a quick process, but it needs extreme temperatures to attain a high diffusion rate for the homogeneous austenitic structure within a short time. For attaining high surface temperature we need high temperature gradient which gives enough heat deep into the material. In a simplified model, in which the heat flow is considered to be one dimensional, the temperature on a depth z and on the surface where $z = 0$ is given by Carslaw and Jeager (1978) as:

$$T_{z,t}=\frac{AI}{k}\sqrt{4\alpha t}\,\mathrm{ierfc}\sqrt{\frac{z^2}{4\alpha t}} \quad (3)$$

where 'A' is absorptivity, 'I' is laser power density in W/m^2 and α is thermal diffusivity.

The surface temperature T_s is given in equation (4).

$$T_s=\frac{AI}{k}\sqrt{\frac{4\alpha t}{\pi}} \quad (4)$$

For a given maximum surface temperature and a hardening depth z (where the temperature is just the Ac_3 temperature) the interaction time t_i, can be solved from equation (5).

$$\frac{T_{AC_3}}{T_s}=\sqrt{\pi}\,\mathrm{ierfc}\sqrt{\frac{z^2}{4\alpha t_i}} \quad (5)$$

The required (absorbed) power density is solved by the following equation

$$AI = T_s k \sqrt{\frac{\pi}{4\alpha t_i}} \tag{6}$$

When the interaction time is of the same order or larger compared to the thermal time constant $R^2/4a$ three-dimensional solution is required. The temperature distribution caused by a stationary laser beam with a uniform power density distribution on a circular spot with radius *R*, is given by:

$$T_{z,t} = \frac{AI}{k}\sqrt{4\alpha t}\left\{\text{ierfc}\sqrt{\frac{z^2}{4\alpha t}}\text{ierfc}\sqrt{\frac{z^2+R^2}{4\alpha t}}\right\} \tag{7}$$

where it is assumed that the workpiece dimensions are large enough for self quenching. The surface temperature at the end of the laser beam interaction follows from:

$$\frac{AI}{k}\sqrt{4\alpha t_i}\left\{\sqrt{\frac{1}{\pi}} - \text{ierfc}\sqrt{\frac{R^2}{4\alpha t_i}}\right\} \tag{8}$$

With a hardening depth *z*, where the maximum temperature equals Tac_3 the interaction time can be solved from the equation (9) (Meijer and Sprang, 1991).

$$\frac{T_{ac3}}{T_s} = \frac{\text{ierfc}\left(z/\sqrt{(4\alpha t_i)}\right) - \text{ierfc}\left(\sqrt{Z^2+R^2}\Big/(4\alpha t_i)\right)}{1/\pi - \text{ierfc}\left(R/\sqrt{4\alpha t_i}\right)} \tag{9}$$

Heat conduction plays an important role in LSH. The classical Fourier's law of heat conduction is used to explain the laser surface treatment and the equation is represented

$$\rho c \frac{\partial T}{\partial t} = \nabla.(k\nabla T) + \rho \dot{q} \tag{10}$$

where ∇T is the time step and $\dot{q}$ the rate of internal energy generated per unit mass. In this, the heat energy losses due to convection and radiation can be neglected during laser transformation hardening (Wu et al., 2006). Ashby and Easterling (1984) developed an approximate solution to the equations of heat flow and combined with kinetic models to find out the near-surface structure and hardness of plain carbon steels after laser treatment. At a point below, the centre of the beam, the temperature field *T*(*z*, *t*) is given by

$$T(z,t) = T_0 + \frac{Aq/v}{2\pi k\left[t\left(t+t_0\right)\right]^{\frac{1}{2}}} \times \exp\left(\frac{\left(z+z_0\right)^2}{4\alpha t}\right) \tag{11}$$

where *k* is the thermal conductivity, '*α*' the thermal diffusivity, '*A*' the absorptivity of the surface (the fraction of the incident energy which is absorbed) and *t* is the time. The constant t_0 measures time for heat to diffuse over a distance equal to the beam radius and the length z_0 measures the distance over which heat can diffuse during the beam interaction-time.

$$t_0 = \frac{r_B^2}{4\alpha} \tag{12}$$

$$z_0 = \frac{r_B}{v} \tag{13}$$

where r_B is the radius of laser beam in meter, v is the tracking velocity (m/s). It is found that steels with carbon content below about 0.1 weight % do not respond to transformation hardening. The hardness of the martensite increases with its distance below the surface, because its carbon content is greatest when the peak temperature is just above Ac_1. The ferrite hardness is practically constant. By measuring the volume fraction, f_m, of the martensitic phase (using a point counting method) the microhardness of the sample could be estimated fairly well from simple rule-of-mixtures.

$$H_v(mean) = f_m H_m + \left(1 - f_m\right) H_f \tag{14}$$

where H_v is the Vickers hardness of the laser-treated surface, H_m is the mean micro hardness of the martensite, H_f is the ferrite at the depth.

When laser beam is focused on specimen the restoration of high density light energy into heat energy is irradiated on specimen, that is, heat input capacity. At this time, the value of heat input capacity was calculated by the following equation.

$$E = \frac{P}{\delta(a/b)V_{ts}} \tag{15}$$

where E, P, δ, a, b and V are the heat input capacity, the power of the laser, the depth of the hardened area, the minor axis of the focus, the major axis of the focus, and the travel speed (V_{ts}) of the laser, respectively (Shin and Yoo, 2008).

2.3 Numerical analysis

Numerical analyses of the hardening process have been carried out by many researchers in recent years to study the temperature and hardness before experimentation. The LSH depends on two thermal cycles: i.e., rapid heating over certain 'transformation temperature' followed by a rapid cooling rate produced on the metals surface exposed to the scanning laser beam. The hardening of the steel depends on the temperature-dependent phase changes of iron and the changes in carbon solubility caused by this transformation during the heating and cooling cycles. Therefore, this process involves solid-state thermal transformations without melting of the metal surface (Chiang and Chen, 2005). Yanez et al. (2002) modelled a numerical solution for the LH process using the finite element code ANSYS to solve the heat transfer equation inside the treated rings made of A420 stainless steel. They proposed a model which includes the temperature dependent thermal properties and the thermal evolution of the boundary conditions. It was concluded that knowledge of the thermal cycles has enabled suitable processing parameters to be ascertained thus improving surface properties when metallic components are irradiated.

The effect of heating rate and cooling rate on the time-dependent temperature fields and phase transformations within the affected zone was investigated by Miokovic et al. (2006). Shercliff and Ashby (1991) developed an approximate heat flow model to predict the case depth in laser transformation hardening of steel surfaces. The model exploits the dimensional relationships between the process variables to produce master diagrams for the hardened depth using Gaussian source. Critical values of dimensionless parameters were found out which predict the conditions for first hardening and the onset of surface melting.

Figure 7 Schematic of LH process showing the temperature survey cross section and the location of each survey point

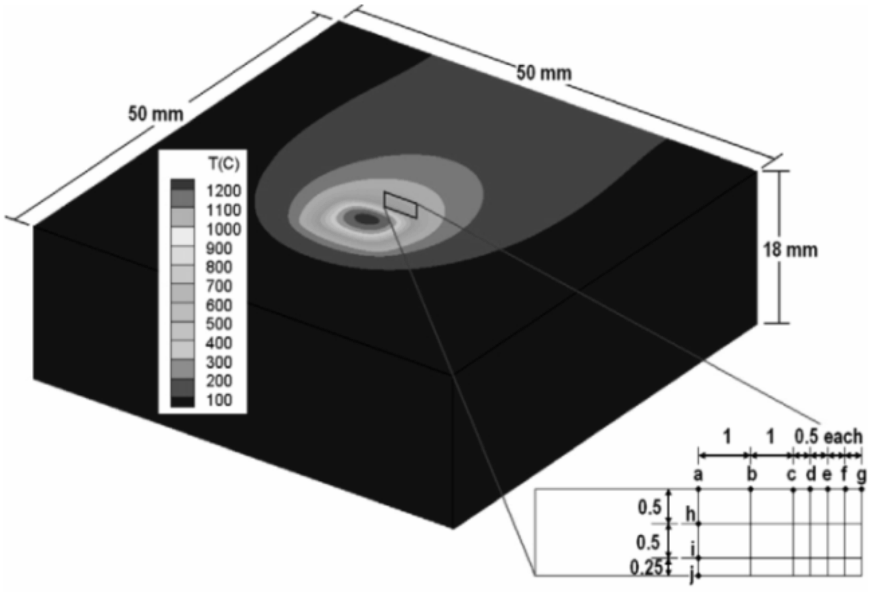

Source: Bailey et al. (2009)

Bailey et al. (2009) designed a predictive model for residual stresses induced in a laser hardened work piece of AISI 4140 steel. They employed the ABAQUS software to make a three-dimensional stress model to predict residual stresses. The phase transformation strains are summed up to the thermal strains at each time step during the heating and cooling cycles to obtain the resultant residual stresses in the work piece. Their model predicted strong compressive residual stresses of about 200MPa in the heat affected zone due to transformation of austenite to martensite. The temperature histories are collected at ten survey points, as shown in Figure 7. The temperatures at all of these survey points go above the Ac_1 temperature where the pearlite transforms to austenite. All points, except *j* and *g*, are also heated above Ac_3 austenisation point, where the remaining ferrite also transforms to austenite. At this point of time, the material at *j* and *g* has a mixed microstructure of austenite and ferrite which depends on the temperature and carbon diffusion. The temperature at survey points *j* and *g* drops sufficiently fast to avoid bainite formation. But since the temperature at these points did not peak over the austenisation temperature and not all ferrite transformed into austenite, there will be residual ferrite that will soften the material at these points.

Figure 8 Prediction of temperature evolution as a function of laser power (470 W) and 5 mm/s of scanning speed

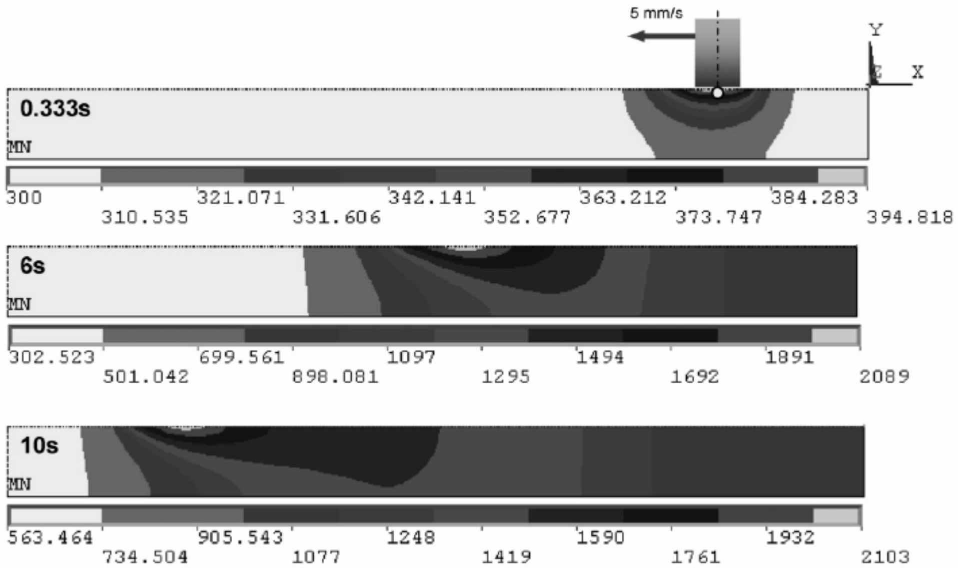

Note: Isotherms at different times: 0.333, 6 and 10 s.

Source: Lusquinos et al. (2007)

Wang et al. (2006) numerically simulated the temperature field in the LH process by MSC. Marc software which used Galerkin method to solve the instantaneous heat transfer equation and they analysed the influence of energy density on LH effect. They verified the simulation result through the thermocouple temperature transducer measuring the specimen surface temperature under the laser irradiation. The temperature distribution of AISI 1045, induced by high power diode laser was obtained by solving the heat conduction equation using the finite element method.

Laser scanning speed of 5, 10 and 15 mm/s were used under variant laser powers: 470, 650 and 760 W. Figure 8 shows the thermal map for a 470 W of laser power and for a scanning speed of 5 mm/s. It is observed that the superficial temperature is not constant along the processed track when the laser beam power was kept constant which is due to the progressive heating of the substrate in front of the laser beam during the processing time. Thus, the laser power should be decreased during the experiment in order to keep constant surface temperature and to produce the uniform hardness on the surface (Lusquinos et al., 2007).

2.4 Material characterisation

Micro hardness testing is the most commonly used testing method for heat treated parts; however, additional tests (such as impact and tensile tests) are required for some critical parts. In some cases, the microstructure of heat-treated parts should be examined under a metallurgical microscope because any property change during heat treatment is closely related to the microstructural change. The microstructural measurements are needed in order to obtain a more informative and quantitative result. These can be done manually; however, an image analyser is used to accomplish the quantitative analysis of microstructures during the last three decades. In LSH, the mechanical and structural properties of the bulk are retained as before, because of the high temperature gradient and high rate of change of temperature that are unattainable by conventional methods (Shang, 1990).

The starting temperature at which austenite begins to forms in equilibrium conditions is the Ac_1 temperature. The temperature at which, the complete transformation to austenite is the Ac_3 temperature. The designations Ac_1 and Ac_3 are used to represent the critical temperatures (Pantsar, 2007). The basic layer of the laser hardened steels consists mainly of pearlite with some ferrite. When the temperature is increased above the critical condition, the steel surfaces are finely heated and the pearlite gets converted into austenite by simultaneous dissolution of the ferrite and cementite constituents. The conduction of heat into the workpiece transforms the austenite into martensite, which is required by successful laser transformation hardening (Basu et al., 2007). Therefore, the austenitising process during laser heating is more important, as this will affect the structures and properties of the subsequent martensite structures. In addition to diffusion transformation of austenite, non-diffusion transformation will also appear, if the temperature is very high with sufficient heating speed (Chen et al., 1997).

Various assumptions are suggested to explain the increased content of retained austenite phase after LH. Fedosov (1999) measured the quantity of the austenite phase by X-ray diffraction. It was concluded that at relatively low temperatures, the increase of retained austenite content was due to the effect of an increased dislocation density.

After the laser treatment, different zones within the surface area occurred as shown in Figure 9. At the top region, a completely martensitic structure develops, which called as the HZ. The transition zone (TZ) consists of partly austenised and eventually hardened microstructure, and the rest is base material which did not transform during the laser irradiation. Depending on the state of the base material, a heat-affected zone can be observed, and underneath this the unaffected base material.

Figure 9 Different zones of laser transformation hardening

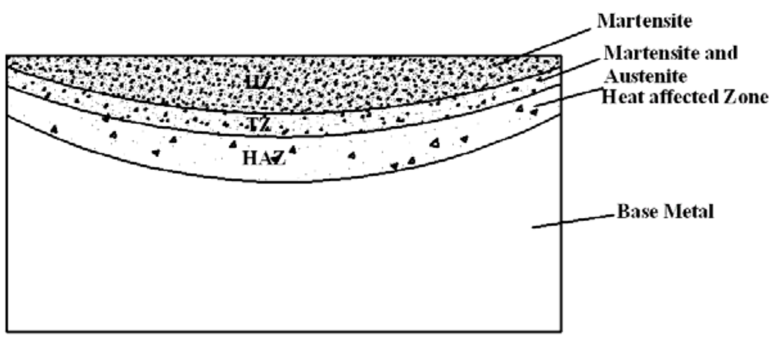

The significance of doing microstructure evaluation is to calculate the grain size, porosity and bonding evaluation, development of interfaces on reaction, crack development in the surface. Higher magnification SEM analysis is used to measure the homogeneity of the martensite formed in the laser-hardened layer and the amount of carbide precipitation in the rapidly-solidified zone. The microstructure obtained due to laser treatment is analysed using scanning electron microscope as shown in Figure 10. It is observed from Figure 10(a) that fine plate martensites, pointing out in different directions, are formed in

0.46% C steel near the surface which is the most hardened structure. Similarly, lathe martensite structure is observed in the case of 0.28% C steel specimen near the surface as shown in Figure 10(b). (Obergfell et al., 2003)

Figure 10 (a) Fine plate martensite in 0.46% C steel (b) lath martensite in 0.28% C steel

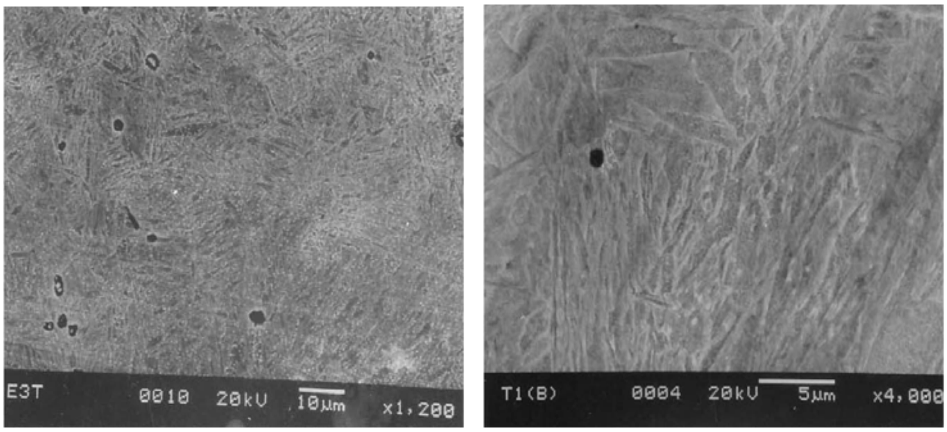

(a) (b)

Source: Obergfell et al. (2003)

Figure 11 A scheme of a hypo-eutectoid microstructure

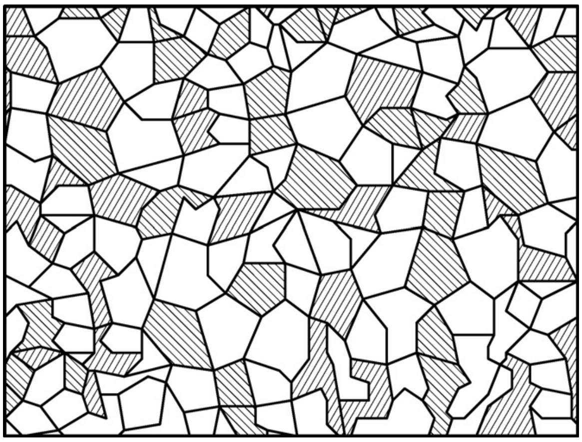

Source: Orazi et al. (2010)

Kaula et al. (2005) aimed at characterisation of dry sliding wear resistance of laser surface hardened En8 steel specimens and compared with the conventionally hardened surface. A 2.5 kW continuous wave CO_2 laser system was used. Their experiment clearly explained that wear rate was critically dependent on the oxide film of the surface which is further influenced by testing parameters as well as dynamic conditions during the course of testing. Under the practical conditions of dry sliding wear, laser surface hardened En8 steel specimens possess superior wear resistance than conventionally hardened specimens.

Orazi et al. (2010) obtained a new austenisation model which depends on the assumption that the pearlite to austenite transformation time is statistically spread out in the microstructure. Each pearlitic colony dissolves in austenite subjected under different temperature/time cycle. Moreover the transformation hysteresis depends on grain size and pearlite coarsening into the grain. Hence, for each grain the austenitic transformation occurred at different temperatures. Considering the schematisation of hypo eutectoid steel as shown in Figure 11, the hatched areas shows that pearlitic colonies while the white one represents ferritic grains.

Figure 12(a) shows the macrostructure of a laser-hardened En18 medium-carbon steel for 1.5 kW CO_2 laser power with an interaction time of 0.18 seconds. A hardened depth of 0.65mm was found using optical microscope. The macrostructure consists of three different regions:

1 the base-metal structure of pearlite and ferrite

2 the adjacent partially-transformed zone

3 the highly-hardened martensite region.

Figure 12 (a) The macrostructure (b) the microstructure at the top surface and at the central region of the laser-HZ; for 1.5 kW CO_2 laser power with an interaction time of 0.18 seconds

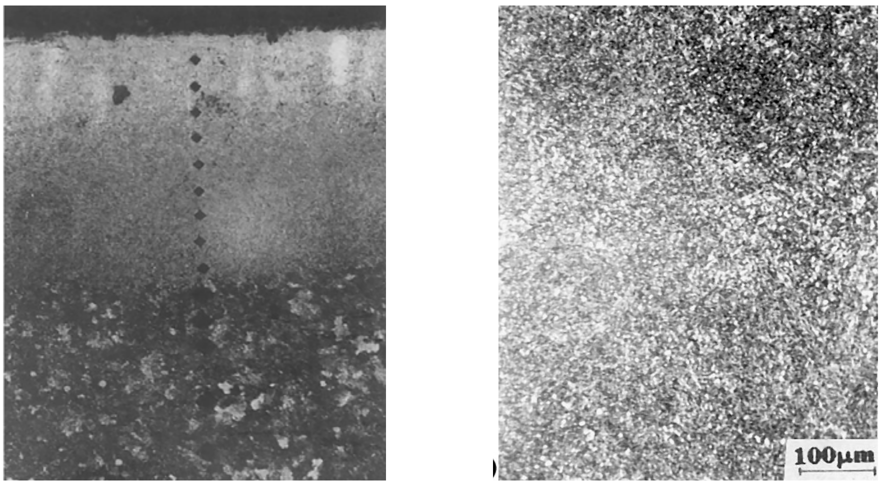

(a) (b)

Source: Senthil Selvan et al. (1999)

Figure 12(b) shows the microstructure observed at the top surface region and the central region of the laser-HZ, consisting of a homogenous martensite layer (Senthil Selvan et al., 1999)

The microstructure investigated in the cross-section of a heat treated En24 steel sample is shown in Figure13. The top dark region resembles the martensite region (Steen, 1991). Discussing about the drawbacks of LH is that it may be necessary to make several passes with the laser over the surface of the work piece if the beam spot size is not large enough to cover the whole area. Lateral heat flow into the previously hardened track may cause 'back tempering' which can reduce the hardness in the affected area considerably.

Figure 13 Microstructure of laser transformation hardened En24 steel

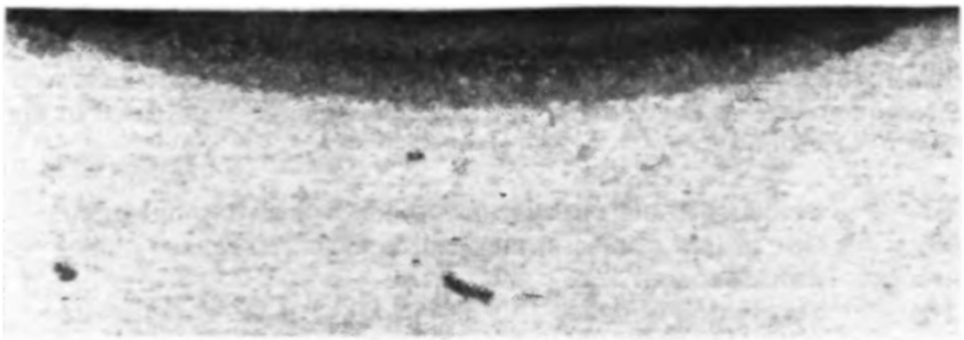

Source: Steen (1991)

3 Conclusions

The following important observations are derived from the review:

1. The microstructure of the surface after laser treatment was finer and more homogenous in comparison with the untreated material.
2. The micro hardness of the steel specimens increases to a greater extent after laser surface treatment.
3. Wear tests revealed the improved wear resistance of the laser treated specimens in comparison with the untreated one. The wear resistance of the surface hardened steel has better wear resistance compared to conventionally hardened material.
4. Monitoring the thermal phenomena at the interaction spot between the laser beam and the material is used for efficient control of LH technique.
5. Design of experiments can be used to optimise the process parameters to obtain the required hardness and depth of HZ.
6. The temperature distribution induced by the laser sources can be obtained by solving the heat conduction equation in finite element method using commercial softwares such as ANSYS, ABAQUS. This analysis reduces the number of experiments and production cost and also save the time.

References

Ashby, M.F. and Easterling, K.E. (1984) 'The transformation hardening of steel surfaces by laser beams-1 hypo-eutectoid steels', *Acta Metallurgica*, Vol. 32, pp.1935–1948.

Bailey, N.S., Tan, W. and Shin, Y.C. (2009) 'Predictive modeling and experimental results for residual stresses in laser hardening of AISI 4140 steel by a high power diode laser', *Surface & Coatings Technology*, Vol. 203, pp.2003–2012.

Basu, A., Chakraborty, J., Shariff, S.M., Padmanabham, G., Joshi, S.V., Sundararajan, G., Dutta Majumdar, J. and Manna, I. (2007) 'Laser surface hardening of austempered (bainitic) ball bearing steel', *Scripta Materialia*, Vol. 56, pp.887–890.

Carslaw, H.S. and Jeager, J.C. (1978) *Conduction of Heat in Solids*, London.

Chen, T.L., Guan, Y.H., Wang, H.G. and Zhang, J.T., (1997) 'A study on austenite transformation during laser heating', *Journal of Materials Processing Technology*, Vol. 63, pp.546–549.

Cheung, N., Pinto, M.A., Ierardi, M.C.F. and Garcia, A. (2004) 'Mathematical modeling and experimental analysis of the hardened zone in laser treatment of a 1045 AISI Steel', *Materials Research*, Vol. 7, pp.349–354.

Chiang, K.A. and Chen, Y.C. (2005) 'Laser surface hardening of H13 steel in the melt case', *Materials Letters*, Vol. 59, pp.1919–1923.

Davis, J.R. (2002) *Surface Hardening of Steels: Understanding the Basics*, ASM International.

Esa, V., David, P., Jonas, L. and Braham, P. (2007) 'Wear characteristic of surface hardened ausferritic Si-steel', *Proceedings of Sino-Swedish Structural Materials Symposium*, pp.245–248.

Fedosov, S.A. (1999) 'Laser beam hardening of carbon and low alloyed steels: discussion of increased quantity of retained austenite', *Journal of Materials Science*, Vol. 34, pp.4259–4264.

Grum, J. and Sturm, R. (1997) 'Laser surface melt-hardening of gray and nodular irons', *Applied Surface Science*, Vols. 109/110, pp.128–132.

Grum, J. (2007) 'Comparison of different techniques of laser surface hardening', *Journal of Achievements in Materials and Manufacturing Engineering*, Vol. 24, No. 1, pp.17–25.

Hirogaki, T., Nakagawa, H., Hayamizu, M., Kita, Y. and Kakino, Y. (2001) 'In-situ heat treatment system for die steels using YAG laser with a machining center', *Journal of the International Societies for Precision Engineering and Nanotechnology*, Vol. 25, pp.212–217.

Hua, M., SeDao, Shao, T.M. and Tam, H.Y. (2007) 'Surface transformation of DF-2 steel after continuous mode laser irradiation', *Journal of Materials Processing Technology*, Vols. 192–193, pp.89–96.

Hwang, J.H., Lee, Y.S., Kim, D.Y. and Youn, J.G. (2002) 'Laser surface hardening of gray cast iron used for piston ring', *Journal of Materials Engineering and Performance*, Vol. 11, pp.294–300.

Kaula, R., Ganesh, P., Tiwari, P., Nandedkar, R.V. and Nath, A.K. (2005) 'Characterization of dry sliding wear resistance of laser surface hardened En8 steel', *Journal of Materials Processing Technology*, Vol. 167, pp.83–90.

Lakhkar, R.S., Shin, Y.C. and Krane, M.J.M. (2008) 'Predictive modeling of multi-track laser hardening of AISI 4140 steel', *Materials Science and Engineering A*, Vol. 480, pp.209–217.

Liu, Q., Song, Y., Yang, Y., Xu, G. and Zhao Z. (1998) 'On the laser quenching of the groove of the piston head in large diesel engines', *Journal of Materials Engineering and Performance*, Vol. 7 pp.402–406.

Lusquinos, F., Conde, J.C., Bonss, S., Riveiro, F. Quintero, A., Comesana, R. and Pou, J. (2007) 'Theoretical and experimental analysis of high power diode laser (HPDL) hardening of AISI 1045 steel', *Applied Surface Science*, Vol. 254, pp.948–954.

Meijer, J. and Sprang, I.V. (1991) 'Optimisation of laser beam transformation hardening by one single parameter', *Annals of the CIRP*, Vol. 40, No. 1, pp.183–186.

Miokovic, T., Schulze, V., Vohringer, O. and Lohe, D. (2006) 'Prediction of phase transformations during laser surface hardening of AISI 4140 including the effects of inhomogeneous austenite formation', *Materials Science and Engineering A*, Vols. 435–436, pp.547–555.

Obergfell, K., Schulze, V. and Vohringer, O. (2003) 'Classification of microstructural changes in laser hardened steel surfaces', *Materials Science and Engineering*, Vol. 355, pp.348-356.

Orazi, L., Fortunato, A., Cuccolini, G. and Tani, G. (2010) 'An efficient model for laser surface hardening of hypo-eutectoid steels', *Applied Surface Science*, Vol. 256, pp.1913–1919.

Pantsar, H. (2007) 'Relationship between processing parameters, alloy atom diffusion distance and surface hardness in laser hardening of tool steel', *Journal of Materials Processing Technology*, Vol. 189, pp.435–440.

Pashby, I.R., Barnes, S. and Bryden, B.G. (2003) 'Surface hardening of steel using a high power diode laser', *Journal of Materials Processing Technology*, Vol. 139, pp.585–588.

Rana, J., Goswami, G.L., Jha, S.K. Mishra, P.K. and Prasad, B.V.S.S.S. (2007) 'Experimental studies on the microstructure and hardness of laser-treated steel specimens', *Optics and Laser Technology*, Vol. 39, pp.385–393.

Ready, J.F. (1997) *Industrial Applications of Lasers*, 2nd ed., Academic Press.

SeDao, Hua, M., Shao, T.M. and Tam, H.Y. (2009) 'Surface modification of DF-2 tool steel under the scan of a YAG laser in continuously moving mode', *Journal of Materials Processing Technology*, Vol. 209, pp.4689–4697.

Senthil Selvan, J. Subramanian, K. and Nath, A.K. (1999) 'Effect of laser surface hardening on En18 (AISI 5135) steel', *Journal of Materials Processing Technology*, Vol. 91, pp.29–36.

Shang, H.M. (1990) 'On the width and depth of hardened zones during laser transformation hardening of tool steels', *Journal of Materials Processing Technology*, Vol. 23, pp.65–72.

Shercliff, H.R. and Ashby, M.F. (1991) 'The prediction of case depth in laser transformation hardening', *Metallurgical Transactions*, Vol. 22, pp.2459–2466.

Shin, H.J. and Yoo, Y.T. (2008) 'Microstructural and hardness investigation of hot-work tool steels by laser surface treatment', *Journal of Materials Processing Technology*, Vol. 201, pp.342–347.

Shiue, R.K. and Chen, C. (1992) 'Laser transformation hardening of tempered 4340 steel', *Metallurgical Transactions*, Vol. 23A, pp.163–170.

Slatter, T., Taylor, H., Lewis, R. and King, P. (2009) 'The influence of laser hardening on wear in the valve and valve seat contact', *Wear*, Vol. 267, pp.797–806.

Steen, W.M. (1991) *Laser Material Processing*, London: Springer-Verlag.

Tani, G., Orazi, L. and Fortunato, A. (2008) 'Prediction of hypo eutectoid steel softening due to tempering phenomena in laser surface hardening', *CIRP Annals-Manufacturing Technology*, Vol. 57, pp.209–212.

Tianmin, S., Meng, H. and Yuen, T.H. (2003) 'Impact wear behavior of laser hardened hypoeutectoid 2Cr13 martensite stainless steel', *Wear*, Vol. 255 pp.444–455.

Totten, G.E. (2006) *Steel Heat Treatment: Equipment and Process Design Handbook*, 2nd ed., Taylor and Francis Group.

Wang, X.F., Lu, X.D., Chen, G.N., Hu, Sh.G. and Su, Y.P. (2006) 'Research on the temperature field in laser hardening', *Optics & Laser Technology*, Vol. 38, pp.8–13.

Wu, W., Liang, N.G., Gan, C.H. and Yu, G. (2006) 'Numerical investigation on laser transformation hardening with different temporal pulse shapes', *Surface and Coatings Technology*, Vol. 200, pp.2686–2694.

Xiu-bo, L., Gang, Y., Jian, G., Quan-yi, S., Zhen-guo, Z. and Yi-jie, G. (2007) 'Analysis of laser surface hardened layers of automobile engine cylinder liner', *Journal of Iron and Steel Research, International*, Vol. 14, No. 1, pp.42–46.

Xu, Z., Leong, K.H. and Reed, C.B. (2008) 'Nondestructive evaluation and real-time monitoring of laser surface hardening', *Journal of Materials Processing Technology*, Vol. 206, pp.120–125.

Yanez, A., Alvarez, J.C., Lopez, A.J., Nicolas, G., Perez, J.A., Ramil, A. and Saavedra, E. (2002) 'Modelling of temperature evolution on metals during laser hardening process', *Applied Surface Science*, Vol. 186, pp.611–616.

Yang, B.Q., Zhang, K., Chen, G.N., Luo, G.X. and Xiao, J.H. (2006) 'A quantitative analysis of the effect of laser transformation hardening on crack driving force in steels', *Surface and Coatings Technology*, Vol. 201, pp.2208–2216.

Yang, L.J., Jana, S. and Tam, S.C. (1990) 'Laser transformation hardening of tool-steel specimens', *Journal of Materials Processing Technology*, Vol. 21, pp.119–130.

Yang, L.J., Jana, S. and Tam, S.C. (1991) 'The effects of pre-hardening on the laser transformation hardening of tool steel specimens', *Journal of Materials Processing Technology*, Vol. 25, pp.321–332.

Zhang, X.M., Man, H.C. and Li, H.D. (1997) 'Wear and friction properties of laser surface hardened En31 steel', *Journal of Materials Processing Technology*, Vol. 69, pp.162–166.

Nomenclature

a	Minor axis of the focus, m
b	Major axis of the focus, m
c	Specific heat, J/kg.K
f_m	Martensite volume fraction, m
k	Thermal conductivity, W/m.K
$\dot{q}$	Rate of energy generation, W/m^3
r_B	Radius of laser beam, m
r, z	Cylindrical coordinates, m
t	Time, s
t_i	Interaction time, s
t_0	Time for heat to diffuse, s
v	Tracking velocity, m/s
z_0	Heat Diffusion distance, m
A	Absorptivity, J
E	Heat input capacity, J/s
H	Surface hardness value
H_v	Vickers hardness
H_m	Mean micro hardness
H_f	Depth of ferrite, m
I	Laser power density, W/m^2
P	Laser power, W
R	Radius of beam, m
S	Sliding distance, m
T	Temperature, K
Ts	Surface temperature, K
V	Travel speed of the laser, m/s
α	Thermal diffusivity, W/m.K
δ	Depth of the hardened area, µm
ρ	Material density, kg/m^3
φ	Angle, rad
∇T	Time step, s